Evaluation of Torque Feedback MTPA Control of IPMSMs using Torque Estimation Map in the Magnetic Saturation and Regenerative Regions

Haruka Tominaga [1)] Keiichiro Kondo [2)]
Kazuhiko Matsunami [3)]

1) Waseda University, School of Advanced Science and Engineering, Shinjuku, Tokyo, Japan
E-mail: h183266@ruri.waseda.jp
2) Waseda University, Faculty of Science and Engineering, Shinjuku, Tokyo, Japan
E-mail: kkondo@waseda.jp
3) Suzuki Motor Corporation, Chuo, Hamamatsu, Shizuoka, Japan
E-mail: kmatsunami@hhq.suzuki.co.jp

Interior Permanent Magnet Synchronous Motors (IPMSMs) are widely applied to drive electric vehicles (EVs) because of their higher efficiency. In IPMSMs high currents cause magnetic saturation of the rotor core inductance fluctuations. Further, temperature changes in the permanent magnet of the rotor cause fluctuations in the electromotive force constant. Torque feedback maximum torque per ampere (MTPA) control, which seeks to achieve high-accuracy and low-loss torque control, necessitates accurate torque estimation and MTPA angle calculation. Conventionally, the accuracy of this control strategy deteriorates because of the parameter fluctuations. In this study, the strategy was applied in conjunction with a torque estimation map that compensates for parameter variations in magnetic saturation and regenerative brake regions.

KEY WORDS: Interior Permanent Magnet Synchronous Motor (IPMSM), Maximum Torque per Ampere Search Method, Torque Feedback Control, Magnetic Saturation, Permanent Magnet Temperature

1. INTRODUCTION

In recent years, the electric-vehicle market has expanded toward carbon neutrality. EVs have issues such as a shorter driving range even with full charge of their battery than internal combustion engine (ICE) driven vehicles with full tank of fuel and longer battery charging times. To solve these issues, it is necessary to improve the efficiency of traction motor drive system. Interior permanent-magnet synchronous motors (IPMSMs) are widely used in EVs because of their high efficiency and high power density. However, the electromotive force constant varies depending on the temperature of the permanent magnets in the rotor, and the inductance varies because of the magnetic saturation of the rotor iron core caused by high current flows. This results in different values for the preset and actual magnetic constants during operation, thereby lowering the steady-state torque output performance and increasing losses.

Many countermeasures for these parameter variations have been proposed. They can be classified between offline and online methods. Offline methods, such as look-up tables (LUTs) [(1)], are performed by analyzing and referring to preliminary experiments. In contrast, online methods entail the development of control systems. Offline methods incur high costs in terms of time, money, and labor because of the need for prior experiments. Online methods perform operations in addition to conventional circuits [(2)]. However, there is an upper limit to the computational load. Therefore, the combination of the two methods has been examined. Specifically, the use of torque feedback maximum torque per ampere (MTPA) control strategy in conjunction with a torque estimation map (Fig. 1) has been proposed to compensate for parameter variations, while incurring low cost and computational load. [(3)]

In this control method, MTPA control, which can output torque at the minimum current vector value, is integrated upstream of the current control system and combined with torque feedback control. In the conventional control strategy [(4)], the current-type torque estimation equation in Equation (1) is differentiated with respect

to the current phase angle. Further, an Equation (2) whose function is zero is used to calculate the MTPA angle.

$$T = P_n\{\Phi_f i_q + (L_d - L_q) i_d i_q \quad \text{..... (1)}$$

$$\theta_{MTPA} = \cos^{-1} \frac{-\Phi_f + \sqrt{\Phi_f^2 + 8(L_d - L_q)^2 I_m^2}}{4(L_d - L_q) I_m} \quad \text{.....(2)}$$

Φ_f: electromotive force constant P_n: number of pole pairs

i_d: d axis flux i_q: q axis flux I_m: current vector

L_d: d axis inductance L_q: q axis inductance θ_{MTPA}: MTPA angle

However, as aforementioned, parameter variations deteriorate the calculation accuracy and increase losses. Therefore, the method entailed the use of i_d, i_q and φ_f obtained online to the torque estimation map obtained offline to perform MTPA angle calculation and torque control, while compensating for parameter variation.

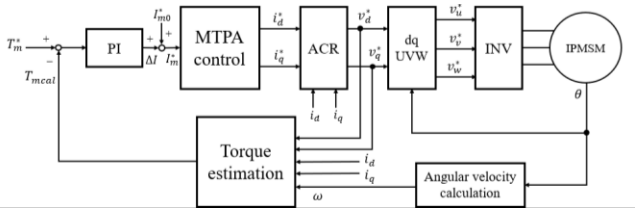

Fig. 1 Block diagram of torque feedback MTPA control

In the previous study [3], the effectiveness of the method was evaluated in regions with small magnetic saturation. In verification of the accuracy of the MTPA angle calculation, compensation of the parameter variation in the direction of the temperature axis was sufficient. However, compensation in the direction of the current axis could not be confirmed. In addition, the accuracy of the MTPA angle calculation and steady-state torque output performance were evaluated only to examine their effectiveness in the motoring regions.

In this study, the MTPA angle calculation accuracy of the method [3] was evaluated based on the copper loss in the region of higher magnetic saturation, and the torque estimation map was extended to the regenerative region. In the regenerative region, the direction of i_q is opposite to that of the motoring region; therefore, the magnetic saturation is different, and the manner in which the inductance fluctuates also changes. Therefore, the effectiveness of the method [3] was evaluated in terms of map acquisition, MTPA angle calculation, and steady-state torque output performance. This study focused on assessing the effectiveness of the method for current-axis parameter variations. In this paper, the method [3] was defined as the proposed method.

2. Maximum Torque per Ampere Search Method using Torque Estimation MAP

2.1. Creation of Torque Estimation MAP

The driving schedule for obtaining the torque estimation map is shown in Fig. 2. The ranges of i_d and i_q were expanded as compared to the previous cases [3], and the objective was to apply them to larger magnetic saturation regions. In addition, the polarity of i_q was reversed, and a separate map was created for application to the regenerative region. The approximation method was the same as that used previously [3].

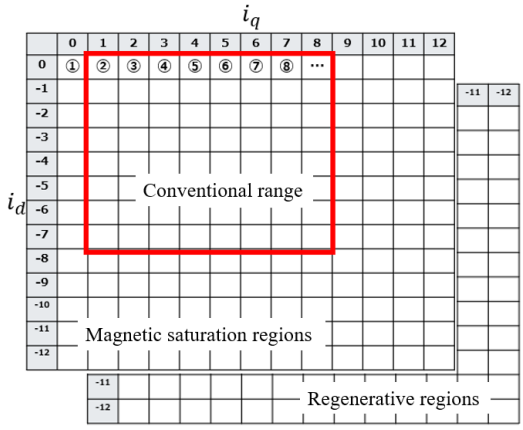

Fig. 2 Driving schedule for map acquisition

2.2. Application of Torque Estimation MAP

In this control strategy, the torque estimation map approximation Equation (3) obtained offline is differentiated with respect to the current phase angle and applied to the MTPA control as shown in Equation (4).

$$T(i_d, i_q) = p00 + p10 * i_d + p01 * i_q + p20 * i_d^2 + p11 * i_d i_q + p02 * i_q^2 \quad \text{..... (3)}$$

$$\frac{-\sqrt{p10^2 + p01^2}}{I_m \sqrt{(p02 - p20)^2 + p11^2}} \sin(\theta_{MTPA} + \alpha) = \sin(2\theta_{MTPA} + \beta) \quad \text{.. (4)}$$

The previous study [3], which focused on the motoring region, calculated the MTPA angle as the intersection of straight lines connecting the minima to the points that moved 1/4 cycle from the minima of the two curves. In the regenerative region, the maxima of the two curves were used instead of the minima.

2.3. Correlation between MTPA Angle Calculation Accuracy and Copper Loss

The MTPA current-vector trajectory is shown in Fig. 3. In the current-type torque estimation equation shown in Equation (2), the parameter variation causes errors in the accuracy of the MTPA angle calculation. Subsequently, the operating point moved along the constant-torque curve. Thus, the current vector value is increased by ΔI compared to the case wherein the exact MTPA angle is calculated.

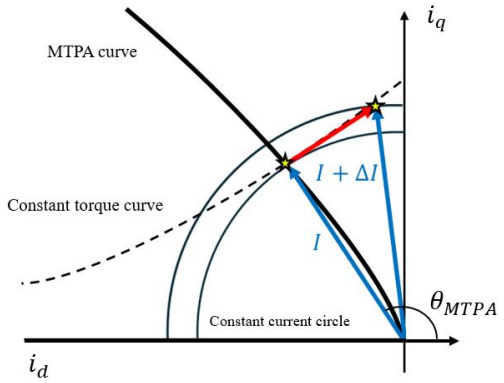

Fig. 3 MTPA current vector trajectory

In other words, the higher the accuracy of the MTPA angle calculation, the smaller would be the current vector value and thus, the smaller would be the copper loss.

2.4. The Performance of Automatic Current Regulator and Parameter Variations

The block diagram of the Automatic Current Regulator (ACR) for torque feedback MTPA control is shown in Fig. 4.

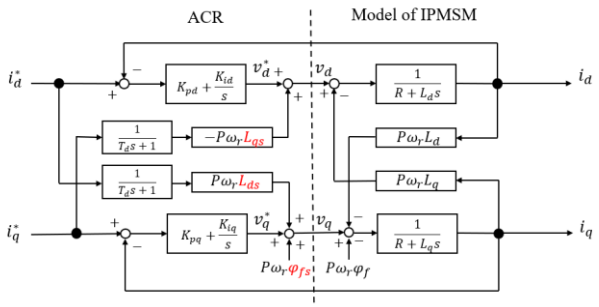

Fig. 4 Block diagram of the Automatic Current Regulator of IPMSMs

The values of inductance and permanent magnet flux coefficient used in the decoupling control are preset to constant values. Therefore, the accuracy of the decoupling control may possibly deteriorate ACR performance due to fluctuations in the motor parameters during its operation. As the result, the step response of the actual torque may become oscillatory rather than a first-order lag system.

3. Evaluation by Experiments Using a Scaled-Down Model

To evaluate the effectiveness of the proposed method for parameter variation, the accuracy of the MTPA angle calculation and steady-state torque output performance were evaluated using a scaled-down model. The parameters of the experimental motor used in the scaled-down model are listed in Table 1. The scaled-down model consisted of a three-pole pair of load IPMSM connected to a two-pole pair of experimental IPMSM via a shaft. A torque meter (UTMII-20Nm) is connected to the shaft.

Table 1 Parameters of the experimental motor

Parameter	Value
DC link voltage	400 [V]
Number of pole pairs	2
Rated power	1.5 [kW]
d-axis inductance	29 [mH]
q-axis inductance	87 [mH]
Winding resistance	1.35 [Ω]
Electromotive force constant	0.234 [Wb]
Rated rotation speed	1500 [rpm]

3.1. Verification of MTPA Angular Calculation Accuracy

The MTPA angle calculation accuracies of the conventional method (Equation (2)) and the proposed method (Equation (4)) were evaluated using the copper loss values calculated from the current vector values. The experimental motor was controlled at a constant speed of approximately 130 [rad/s], and the torque reference value was varied in the range of 4 to 16 [Nm] in the motoring region and -4 to -16 [Nm] in the regenerative region. Table 2 shows the results corresponding to 25 [°C] in the motoring region, and Table 3 shows the results corresponding to 125 [°C]. Table 4 shows the results for 25 [°C] in the regenerative region and Table 5 shows the results corresponding to 125 [°C]. Figures 5 to 8 depict the calculated copper losses for the aforementioned cases, respectively.

Table 2 MTPA angular calculation accuracy [25°C]
(motoring region)

Torque reference [Nm]	4.0	8.0	12.0	16.0
θ_{MTPA}(Proposed approximation method) [deg]	124.2	128.0	129.7	130.8
θ_{MTPA}(Conventional method) [deg]	124.4	129.5	132.0	133.6
I_m^*(Proposed approximation method) [A]	5.839	9.611	12.88	16.00
I_m^*(Conventional method) [A]	5.832	9.583	12.80	15.84
Copper loss(Proposed approximation method) [W]	46.03	124.7	223.9	345.5
Copper loss(Conventional method) [W]	45.91	124.0	221.3	338.8

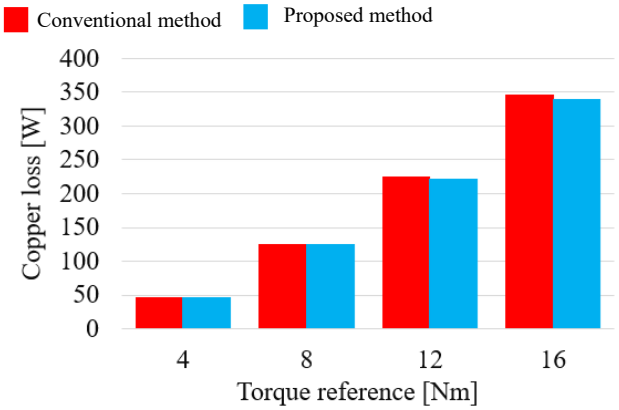

Fig. 5 Comparison of copper losses [25°C]
(motoring region)

Table 3 MTPA angular calculation accuracy [125°C]
(motoring region)

Torque reference [Nm]	4.0	8.0	12.0	16.0
θ_{MTPA}(Proposed approximation method) [deg]	124.6	128.4	130.0	131.1
θ_{MTPA}(Conventional method) [deg]	125.5	130.4	132.8	134.4
I_m^*(Proposed approximation method) [A]	5.990	9.793	13.11	16.29
I_m^*(Conventional method) [A]	5.983	9.759	13.01	16.10
Copper loss(Proposed approximation method) [W]	48.44	129.5	231.9	358.4
Copper loss(Conventional method) [W]	48.33	128.6	228.5	350.0

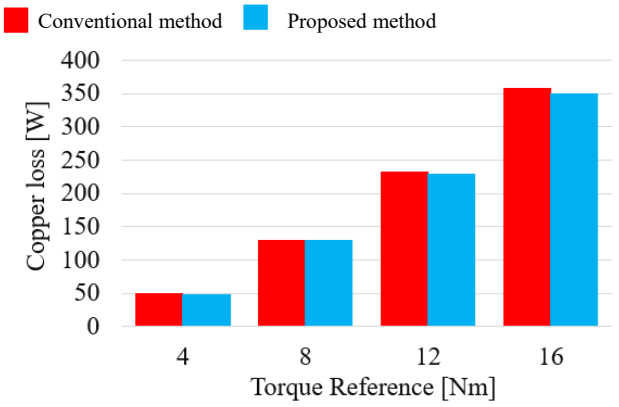

Fig. 6 Comparison of copper losses [125°C]
(motoring region)

Table 4 MTPA angular calculation accuracy [25°C]
(regenerative region)

Torque reference [Nm]	-4.0	-8.0	-12.0	-16.0
θ_{MTPA}(Proposed approximation method) [deg]	237.4	233.5	231.8	230.8
θ_{MTPA}(Conventional method) [deg]	238.9	233.7	230.9	229.1
I_m^*(Proposed approximation method) [A]	5.313	8.550	11.30	13.87
I_m^*(Conventional method) [A]	5.327	8.561	11.30	13.84
Copper loss(Proposed approximation method) [W]	38.11	98.69	172.4	259.8
Copper loss(Conventional method) [W]	38.31	98.95	172.3	258.6

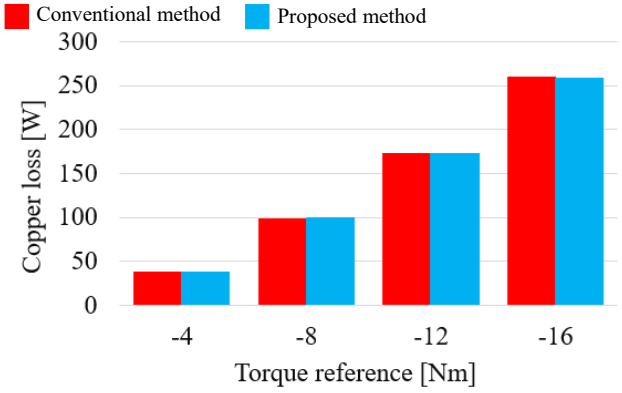

Fig. 7 Comparison of copper losses [25°C]
(regenerative region)

Table 5 MTPA angular calculation accuracy [125°C]
(regenerative region)

Torque reference [Nm]	-4.0	-8.0	-12.0	-16.0
θ_{MTPA}(Proposed approximation method) [deg]	238.2	234.4	232.7	231.6
θ_{MTPA}(Conventional method) [deg]	238.7	233.5	230.7	228.9
I_m^*(Proposed approximation method) [A]	5.470	8.720	11.50	14.10
I_m^*(Conventional method) [A]	5.468	8.716	11.47	14.03
Copper loss(Proposed approximation method) [W]	40.38	102.6	178.5	268.5
Copper loss(Conventional method) [W]	40.37	102.6	177.5	265.7

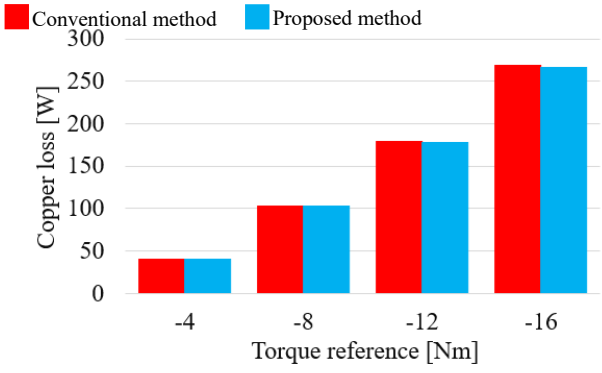

Fig. 8 Comparison of copper losses [125°C]
(regenerative region)

In low torques range, no significant difference was observed in the copper loss between the conventional and proposed methods.

Therefore, the approximation accuracy of the proposed method using the local maximum is high, even in the regenerative region. In addition, the copper loss at high torque of the proposed method is smaller than that of the conventional method because of the compensation for parameter variations in the region of high magnetic saturation. The same trend is observed in the motoring and regenerative regions. As shown in Table 2 and 3, at 25 [°C], a loss reduction effect of up to 6.7 [W] was observed in the motoring region and up to 1.2 [W] in the regeneration region. This means that the proposed method compensates for the fluctuations in inductance and permanent magnet magnetic flux. However, the effect is lower in the regeneration region compared to the motoring region, it results that the accuracy of the torque estimation approximation formula is not so high. But the proposed method can derive the current phase angle by means of the simple equation by using an approximation, obviating complicated formulas such as the once with arccosine. Therefore, the MTPA angle can be calculated with low computational load.

3.2. Verification of Steady-state Torque Output Performance

The steady-state torque output performance was evaluated using the torque feedback MTPA control, as shown in Fig. 1. The experimental motor was controlled at a constant speed of approximately 160 rad/s, and the torque reference value was varied in the range of 4 to 16 [Nm] in the motoring region and -4 to -16 [Nm] in the regenerative region. The error was derived by comparing the torque reference value with the actual torque measured using the torque meter. The conventional method uses Equations (1) and (2) for the torque estimation and MTPA angle calculation, whereas the proposed method uses Equations (3) and (4). The results for the motoring region at 25 [°C] are presented in Table 6 and Fig. 9, and the results at 125 [°C] are presented in Table 7 and Fig. 10. Whereas those for the regenerative region at 25 [°C] are presented in Table 8 and Fig. 11, and the results at 125 [°C] are presented in Table 9 and Fig. 12.

Table 6 Steady-state torque output performance [25°C]
(motoring region)

	Output torque [Nm]		
Torque reference [Nm]	4.0	10.0	16.0
Proposed [Nm]	3.74	10.42	16.20
Conventional [Nm]	3.76	9.30	13.77

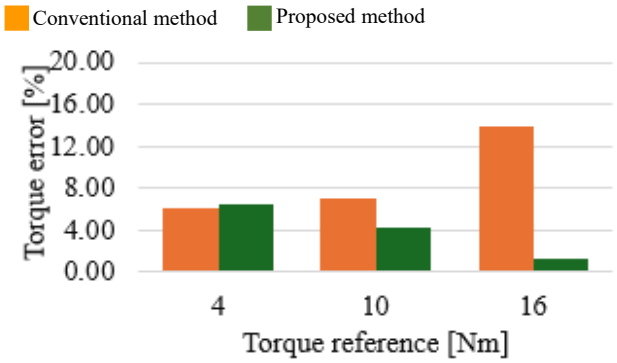

Fig. 9 Output torque error [25°C]
(motoring region)

Table 7 Steady-state torque output performance [125°C]
(motoring region)

	Output torque [Nm]		
Torque reference [Nm]	4.0	10.0	16.0
Proposed [Nm]	3.79	10.51	16.27
Conventional [Nm]	3.68	9.15	13.50

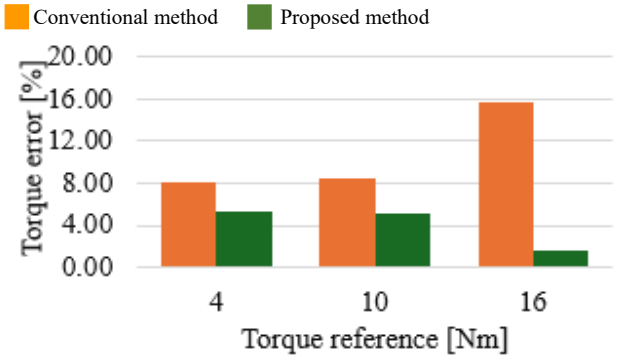

Fig. 10 Output torque error [125°C]
(motoring region)

Table 8 Steady-state torque output performance [25°C]
(regenerative region)

	Output torque [Nm]		
Torque reference [Nm]	-4.0	-10.0	-16.0
Proposed [Nm]	-3.49	-9.17	-14.21
Conventional [Nm]	-4.11	-9.69	-14.07

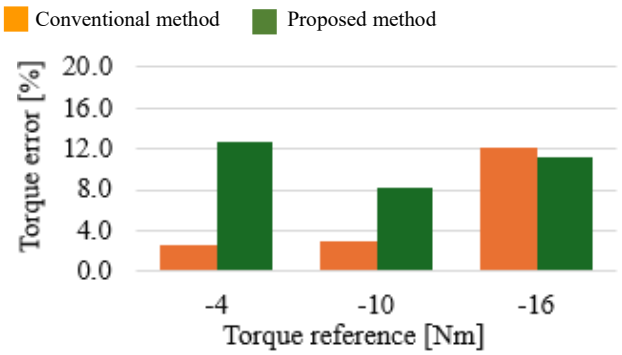

Fig. 11 Output torque error [25℃]
(regenerative region)

Table 9 Steady-state torque output performance [125℃]
(regenerative region)

	Output torque [Nm]		
Torque reference [Nm]	-4.0	-10.0	-16.0
Proposed [Nm]	-3.43	-9.11	-14.07
Conventional [Nm]	-3.89	-9.39	-13.67

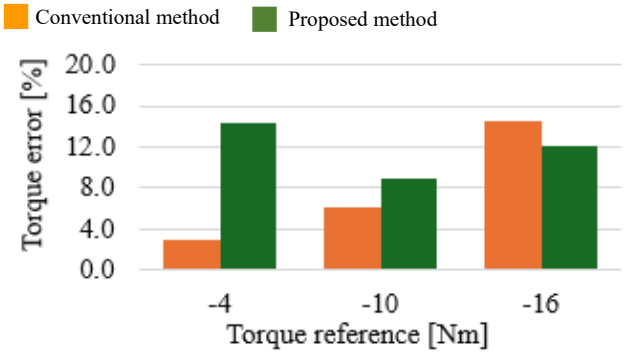

Fig. 12 Output torque error [125℃]
(regenerative region)

In the case of the conventional method, the error increased linearly with the torque in both regions. This is because the inductance fluctuates owing to the magnetic saturation and deviates from the preset value. In contrast, the proposed method compensates for parameter variations and the steady-state torque output performance in high torque region is better than that by the conventional method. Thus, the effectiveness of the proposed method in compensating for parameter variations in regions of high magnetic saturation was confirmed, not only in the motoring region but also in the regenerative region. However, the error of the proposed method was larger in the regenerative region than in the motoring region.

3.3. Verification of Dynamic Torque Control Performance by Torque Step Responses

The dynamic torque control performance of the ACR in the magnetic saturation region are verified by evaluating the torque step response. Both the ACR and the torque feedback control system are set to a first-order lag system with a time constant of 0.01 [s]. The IPMSM for the experimental setup is controlled at a constant speed of 233 [rad/s] by the load motor. An RC filter with a time constant of 0.003 [s] is connected to the analog output of the torque meter. Fig. 13 shows the torque step response waveforms at 4 [Nm].

The actual torque measured by a torque meter shows the speed oscillation caused by the tortional elastic vibration of axle of the motors due to the step change of the IPMSM torque. Therefore, in this paper, the calculated torque by Equation (3) is utilized to evaluate the dynamic electromagnetic torque instead of the actual torque measured by a torque meter. The results at the step change of torque command 0 to 4 [Nm] are shown in Fig. 14, and the results with 0 to 16 [Nm] are shown in Fig. 15.

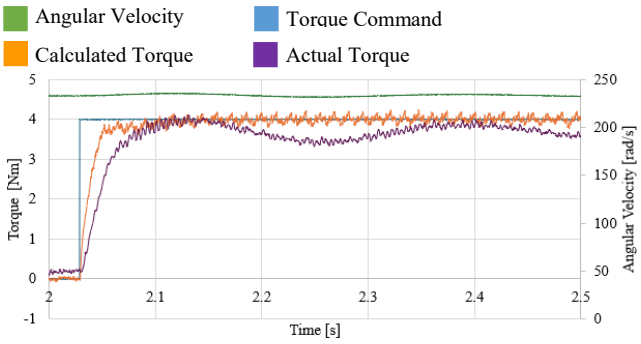

Fig. 13 Actual Torque Step Response Waveform
(Torque Command 4[Nm])

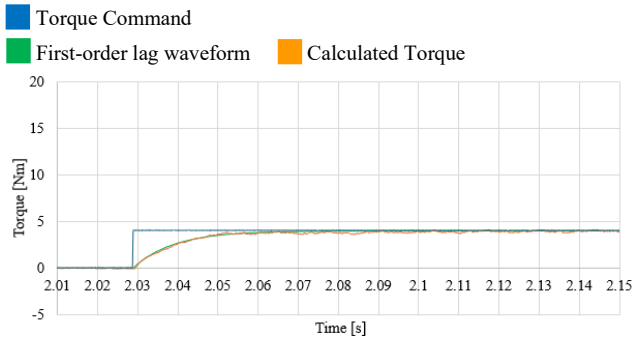

Fig. 14 Torque Step Response Waveform
(Torque Command 4[Nm])

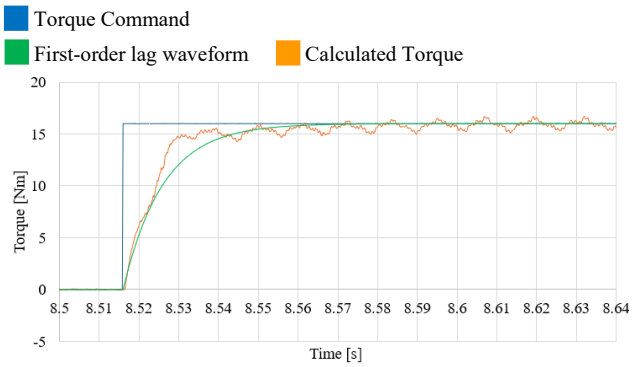

Fig. 15 Torque Step Response Waveform
(Torque Command 16[Nm])

In the step response when the torque command value is low all, the calculated torque waveform almost follows the ideal waveform of the first-order lag system. Thus, it results that ideal decoupling control is achieved. However, when the torque command value is high, the overshoot of the calculated torque waveform shows compared with the ideal first-order lag waveform, and the accuracy of the decoupling control is deteriorated. Therefore, in the ACR for the torque feedback MTPA control, which is the subject of this study, it is considered that dynamic torque control performance deteriorates in the high current region because the decoupling control is not achieved due to the inductance fluctuation caused by magnetic saturation.

4. CONCLUSIONS

In IPMSMs, temperature and current changes affect the electromotive force and inductance, increasing losses and reducing the steady-state torque output performance. This study assessed the efficacy of the use of torque feedback MTPA control in conjunction with torque estimation map to compensate for parameter variations at large magnetic saturations and regenerative regions. The scaled-down model validated the reduction in losses and precise steady-state torque output performance in the magnetic saturation region, thereby demonstrating that the proposed method can be effectively applied to a broader torque range. It is also revealed that the decoupling control in the ACR deteriorates, and the dynamic torque control performance is degraded. Investigations on the mechanism by which the error in the steady-state torque output performance was larger in the regenerative region than in the motoring region is underway.

REFERENCES

(1) B. Cheng, and T.R. Tesch, “Torque Feedforward Control Technique for Permanent-Magnet Synchronous Motors,” *Transactions on Industrial Electronics*, *IEEE*, vol. 57, no. 3, pp. 969-974, March 2010.

(2) S. Sasayama, Y. Shimizu, S. Morimoto, Y. Inoue and M. Sanada, “Maximum Torque per Ampere Control of IPMSM Using Online Flux Linkage Plane Estimation Considering Cross Saturation,” *Journal of Industrial Application, IEEJ*, vol. 12, no. 3, pp. 319-325, Jan 2023.

(3) S. Kawashima, K. kondo and K. Matsunami, “Torque Feedback MTPA Control using an Estimated Torque Approximation Equation,” *Journal of Industrial Application*, *IEEJ*, vol.14, no.1, pp. 47-55, Jan 2025.

(4) H. Hirano, K. Aiso, K. Kondo and K. Matsunami, “Torque Feed-Back MTPA Control for IPMSM Compensating for Magnet Flux Variation Due to Permanent Magnet Temperature,” *2020 23rd International Conference on Electrical Machines and Systems (ICEMS),* pp. 365-368, Hamamatsu, Japan, November 24-27, 2020.